Density Functional Study of Possible Intermediates in the Mechanism of Olefin Cyclopropanation Catalyzed by Metal Carboxylates

Cristóbal Rodríguez-García,[a] Òscar González-Blanco,[a] Antonio Oliva,[a] Rosa M. Ortuño,[a] and Vicenç Branchadell*[a]

Keywords: Carbene complexes / Carboxylato complexes / Density functional calculations / Palladium / Rhodium

The structures of several complexes arising from the interaction between methylene and palladium and rhodium diformates were optimized through density functional calculations. For palladium, mono-, di-, and trimeric complexes were considered. The results obtained show that in all cases the most stable structures correspond to complexes in which methylene has inserted in one of the M–O bonds, while metal–carbene complexes are energy minima only for monomeric palladium diformate and for rhodium diformate. Trimeric palladium formate is thermodynamically stable upon fragmentation. However, when it reacts with methylene, fragmentation becomes favorable. The role of the resulting monomeric complex in the olefin cyclopropanation mechanism catalyzed by palladium dicarboxylates is discussed.

Introduction

The reaction of olefins with diazomethane catalyzed by transition metal complexes is one of the methods for obtaining cyclopropane derivatives.[1–2] The generally accepted mechanism for this reaction involves the formation of a metal–carbene complex as intermediate. Pfeiffer and Dötz[3] have recently reported the first direct spectroscopic observation of such an intermediate for cyclopropanation reactions of enol ethers catalyzed by Cr^0 complexes.

Rhodium and palladium diacetates are among the most efficient catalysts for the cyclopropanation of olefins by diazo compounds. Because their ability to coordinate olefins differs, different mechanisms for these two catalysts have been postulated.[4] For rhodium, the first step would be the formation of the metal–carbene complex that would then react with the olefin, whereas for palladium a metal–olefin complex would be formed before the attack at diazomethane.

Ortuño et al.[5] have reported that in the reaction between diazomethane and chiral cyclohexenones catalyzed by palladium diacetate, the methylenation can take place both at the C–C double bond and at the carbonyl group, the site-selectivity of the process depending on the nature of the substituents in cyclohexenone. The knowledge of the structure of the intermediate arising from the interaction between diazomethane and palladium diacetate seems crucial for understanding the origin of this selectivity.

Metal–carbene complexes have also been studied from a theoretical point of view.[6–13] Vyboishchikov and Frenking[13] have recently studied a series of tungsten–carbene complexes and have analyzed the nature of the bonding. For low-valent complexes, such as $(CO)_5WCH_2$, the bonding can be analyzed in terms of an electron donation from the HOMO of singlet methylene to the corresponding empty d orbital of the metal and a back-donation from one of the doubly occupied dπ orbitals of the metal to the virtual $1b_1$ orbital of singlet methylene. On the other hand, for high-valent complexes, such as Cl_4WCH_2, the bonding is better described as a covalent double bond arising from the interaction between metal and methylene open-shell fragments. In this case, the metal–carbene bond is stronger (larger bond dissociation energy and shorter bond length).

In this paper we present a theoretical study of complexes arising from the reaction between diazomethane and palladium dicarboxylates, which can be relevant in the olefin cyclopropanation mechanism. The alkyl groups have been modeled by hydrogen atoms to simplify the calculations.

Computational Details

Molecular geometries were fully optimized at the generalized gradient approximation (GGA) level of calculation with Becke's[14] exchange potential and the correlation potential of Perdew and Wang[15] (BPW91) implemented in the ADF program.[16–18] The inner electrons of the metal (up to the 3d shell), C, and O were treated within the frozen-core approximation.[17] For the valence space, a basis set of uncontracted Slater-type orbitals was used.[19] The basis set for the metal is triple-ξ. The valence basis set for C, O, and H is of the double-ξ type, supplemented with a set of 3d (C and O) and 2p (H) polarization functions. At this level of calculation the computed bonding energy of $PdCH_2$ is 49.4 kcal mol^{-1}, in excellent agreement with the value obtained by Siegbahn,[20] using the MCPF method (51.0 kcal mol^{-1}).

Relativistic effects were considered in all atoms through the so-called quasi-relativistic method,[21] in which the first-order scalar relativistic Pauli Hamiltonian is diagonalized in the space of the nonrelativistic solutions. These effects were included in the geometry optimization.

[a] Departament de Química,
Universitat Autònoma de Barcelona, Edifici Cn,
08193 Bellaterra, Spain
Fax: (internat.) +34-935812920
E-mail: vicenc@klingon.uab.es

  1434–1948/00/0505–1073 $ 17.50+.50/0

Molecular geometries were also optimized at the local density approximation[22] (LDA) level of calculation with the Gaussian-98 program.[23] These geometries were used to calculate harmonic vibrational frequencies. In these calculations we used the effective core potentials of Hay and Wadt[24] for the metal atoms. For the remaining atoms we used the D95 basis set[25] supplemented with a set of 3d polarization functions for C and O.

Results and Discussion

Palladium diacetate has a trimeric structure in the solid state.[26] We optimized the geometry of trimeric palladium diformate as well as those corresponding to the dimer and the monomer. For comparison, we also studied dimeric rhodium diformate.[27] The optimized geometries of these complexes are shown in Figure 1 and selected geometry parameters are presented in Table 1.

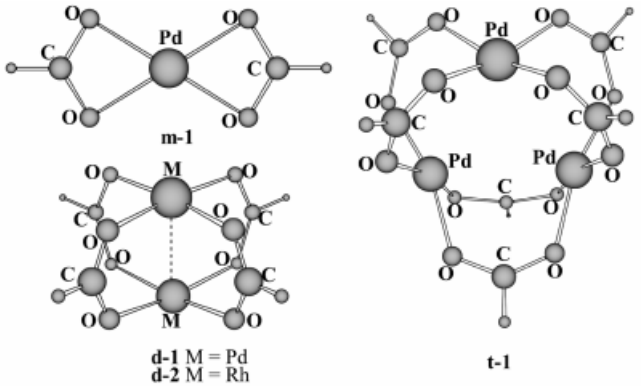

Figure 1. Structures of palladium and rhodium diformates

Table 1. Selected geometry parameters obtained for palladium and rhodium diformate

Structure[a]	M–O[b]	O–C	M–O–C	O–C–O	O–M–O	M–M
m-1	2.082	1.278	89.2	118.2	63.5	
d-1	2.07	1.271	118.1	131.1	89.8	2.581
d-2	2.059	1.270	116.8	128.9	90.0	2.380
t-1[c]	2.049	1.262	127.5	131.5	92.5	3.242
	(1.989)	(1.237)	(130.9)	(125.6)		(3.131)

[a] See Figure 1. – [b] Distances in Å, angles in degrees. – [c] Experimental values corresponding to the crystal structure of palladium diacetate are given in parentheses (ref.[26a]).

Monomeric palladium diformate, **m-1**, has D_{2h} symmetry with the two formate ligands in a bidentate coordination mode, in such a way that Pd is in a square-planar environment, as expected for d^8 ML_4 complexes.

Dimeric palladium diformate, **d-1**, and rhodium diformate, **d-2**, have D_{4h} symmetry. Both metal atoms are linked to each other through four bridging formate ligands, so that each metal atom is also in a square-planar environment. In this environment, Rh^{II} has a d^7 electron configuration. The d orbital pointing to the four oxygen atoms of the coordination plane is empty, while the d_{z^2} orbital, which is perpendicular to the coordination plane, is singly occupied. The interaction between the d_{z^2} orbitals of both Rh atoms leads to a single Rh–Rh bond in **d-2**. The geometry parameters obtained for this complex are very similar to those reported by Cotton and Feng.[28] On the other hand, for the palladium dimeric complex, **d-1**, there is no metal–metal bond, since the dz^2 orbitals of both Pd atoms are doubly occupied. The relatively short value of the Pd–Pd distance is due to the bridging ligands and it is similar to values observed for other Pd^{II} dinuclear complexes.[28]

The trimeric palladium diformate, **t-1**, has D_{3h} symmetry, with the three Pd atoms forming an equilateral triangle (see Figure 1). Two formate bridges link each pair of Pd atoms, leading to a square-planar environment for all metal centers. The optimized geometry parameters obtained for **t-1** (see Table 1) are in very good agreement with the crystal structure determined for palladium diacetate.[26]

Even though palladium diacetate has a trimeric structure in the solid state, in solution it could also exist as a monomer or a dimer. Fragmentation of **t-1** could take place according to the following steps:

t-1 → **d-1** + **m-1** (1)

d-1 → **m-1** + **m-1** (2)

Table 2. Variation of energy and of thermodynamic functions; computed for palladium diformate fragmentation

Step	ΔE[a]	$\Delta H°_{298}$ [a]	$\Delta S°_{298}$[b]	$\Delta G°_{298}$[a]
1	30.9	29.3	43.3	16.4
2	28.1	26.2	48.9	11.6

[a] In kcal mol^{-1}. – [b] In cal K^{-1} mol^{-1}.

Table 2 presents the computed values for energies and thermodynamic functions associated with these steps. Fragmentation of **t-1** is energetically and thermodynamically unfavorable in the gas phase. However, we cannot exclude the possibility that the solvent effect or the coordination of an additional ligand make this process feasible. For this reason, we will consider the formation of carbene complexes from the three forms of palladium diformate.

For comparison, we also considered the fragmentation of **d-2**, which would lead to planar monomeric rhodium diformate in a ^2A_g state. This process is energetically more unfavorable than the fragmentation of **d-1**, the computed fragmentation energy being 80.3 kcal mol^{-1}, since it would involve the cleavage of a Rh–Rh bond, whereas for the palladium complex the metal–metal interaction is repulsive.

For the interaction of methylene with **m-1**, we obtained two different structures (see Figure 2): a Pd–CH_2 complex with C_2 symmetry (**m-3**) and a structure in which methylene has inserted into one of the Pd–O bonds (**m-4**). Both structures are energy minima, since all their vibrational frequencies are real. The **m-3** structure can be considered as a distorted trigonal bipyramid in which O1 and O2 are in the axial positions. The inserted structure **m-4** is 35.3 kcal mol^{-1} more stable than **m-3** and the coordination is square planar.

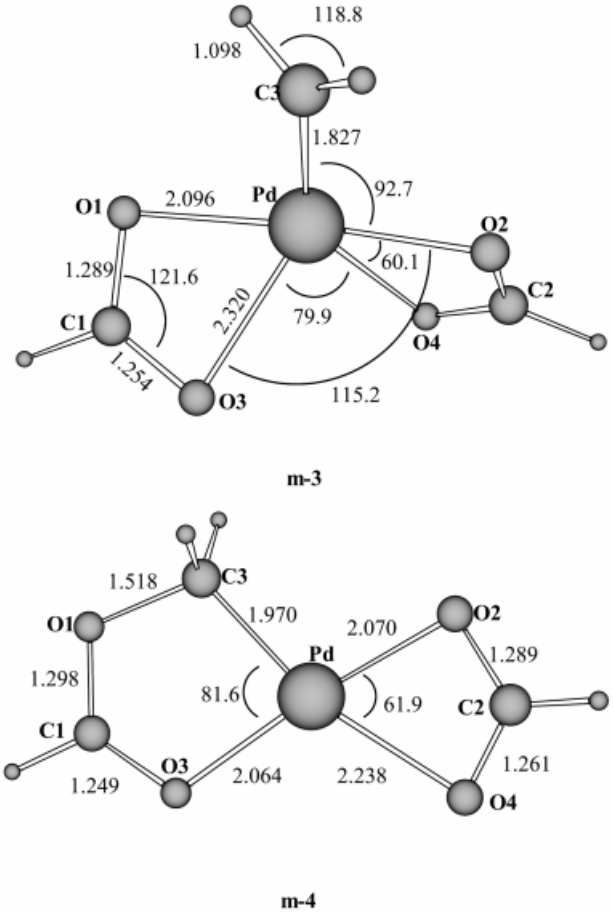

Figure 2. Structures of complexes arising from the interaction between methylene and monomeric palladium diformate; distances are in Å and angles in degrees

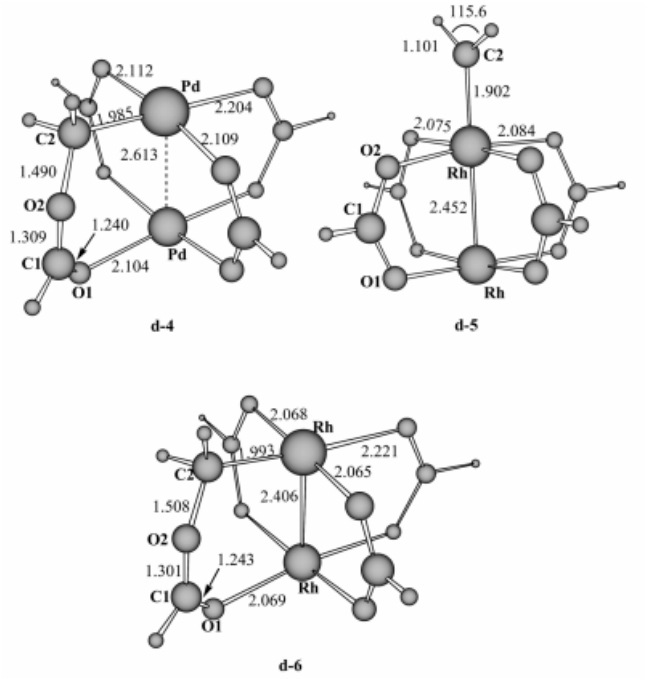

Figure 3. Structures of complexes arising from the interaction between methylene and dimeric rhodium and palladium diformates; distances are in Å and angles in degrees

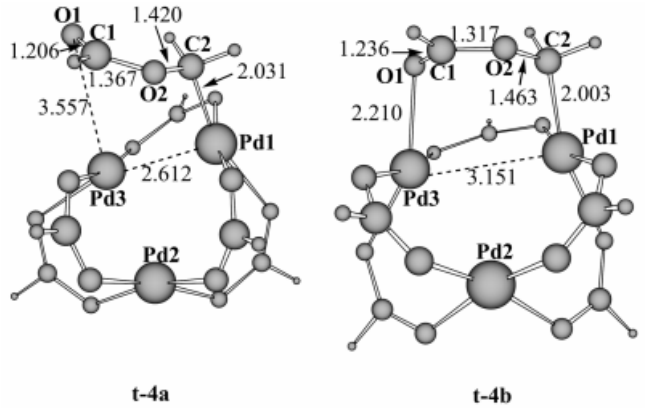

Figure 4. Structures of complexes arising from the interaction between methylene and trimeric palladium diformate; distances are in Å and angles in degrees

Figure 3 represents the structures obtained for the interaction of methylene with dimeric complexes **d-1** and **d-2**. For rhodium diformate, we obtained a metal–carbene complex with C_{2v} symmetry (**d-5**). A similar structure was optimized for palladium diformate, but it has three imaginary frequencies, of symmetries a_2, b_1, and b_2. By lowering the symmetry to C_2, a structure with one imaginary frequency of b symmetry is obtained. Relaxation of all symmetry constraints leads to a structure in which the CH_2 group has inserted into one of the Pd–O bonds (**d-4**). This structure is 35.4 kcal mol^{-1} lower in energy than the C_{2v} Pd–CH_2 structure. A similar CH_2-inserted structure was also obtained for Rh (**d-6**), this structure being 16.6 kcal mol^{-1} lower in energy than **d-5**.

For the interaction between **t-1** and methylene, we obtained a Pd–CH_2 structure with C_2 symmetry. However, this structure is not an energy minimum, since it has an imaginary frequency of b symmetry. When symmetry restrictions are removed, this structure evolves to the CH_2-inserted complex **t-4a** represented in Figure 4. This structure is 32.3 kcal mol^{-1} lower in energy than the C_2 one. Figure 4 shows that in **t-4a** one of the Pd atoms is surrounded by only three oxygen atoms, and that the C1–O1 carbonyl group is not interacting with any of the Pd atoms. We also optimized the geometry of a CH_2-inserted structure in which all Pd atoms are linked through bidentate ligands, as in dimeric complexes **d-4** and **d-6**. The obtained structure, **t-4b**, which is also shown in Figure 4, is 6.0 kcal higher in energy than **t-4a**.

The value of the Pd1–Pd3 distance in **t-4a** (see Figure 4) and the fact that Pd3 is only coordinated to three oxygen atoms seem to indicate that some kind of bonding interaction exists between Pd1 and Pd3. This interaction could be viewed as the electron donation from an occupied dz^2-type orbital perpendicular to the Pd1 coordination plane to an empty d orbital of Pd3. In this way, Pd3 would be in a square-planar tetracoordinated environment, while Pd1 would be in a square-pyramidal pentacoordinated environment.

Structure **t-4b** would be more similar to the CH_2-inserted structures obtained for the monomer and the dimer. However, it is destabilized with respect to **t-4a**. The reason is that the Pd1–Pd3 distance is too large for a bridging ligand such as CH_2OCHO. In the monomeric complex **m-4**, all the C and O atoms of the CH_2OCHO bidentate ligand are in the same plane as Pd, so that the C1–O1–C3–Pd dihedral angle is 0°. In the dimeric complexes, the CH_2OCHO bridging ligand is not coplanar with the metal atoms and the C1–O2–C2–M dihedral angle is –59.4° for **d-4** (M = Pd) and –57.8° for **d-6** (M = Rh). Finally, in **t-4b**, the C1–O2–C2–Pd1 dihedral angle is –80.1°. This large deviation from planarity makes **t-4b** unstable with respect to **t-4a**.

These results suggest that a metal–carbene complex does not exist for dimeric and trimeric palladium dicarboxylates. This kind of structure would exist for monomeric palladium dicarboxylates and for dimeric rhodium dicarboxylates, but, in both cases, the metal–carbene complex would be unstable with respect to methylene insertion in one of the M–O bonds. To rationalize these results, we will analyze the metal–carbene bond in complexes **m-3** and **d-5**.

For comparison, we also optimized the geometries of $(CO)_5WCH_2$ and Cl_4WCH_2 as representative examples of different kinds of metal–carbene complexes. The results obtained, which are summarized in Table 3, are very similar to those reported by Vyboishchikov and Frenking.[13] If we compare the values of the M–CH_2 bond length and of the internal geometry parameters of the methylene group corresponding to **m-3** (Figure 2) and **d-5** (Figure 3) with those

Table 3. Selected geometry parameters of $(CO)_5WCH_2$ and Cl_4WCH_2

Complex	Geometry parameter[a]	
$(CO)_5WCH_2$	W–C[b]	2.070
	C–H	1.101
	H–C–H	108.9
Cl_4WCH_2	W–C	1.881
	C–H	1.097
	H–C–H	115.6

[a] Bond lengths in Å and bond angles in degrees. – [b] Methylene C atom.

presented in Table 3, we observe that Pd and Rh complexes are more similar to Cl_4WCH_2 than to $(CO)_5WCH_2$. So, **m-3** and **d-5** complexes would be better viewed as arising from the interaction of the $^3B_1$ ground state of methylene with the corresponding metal fragment also in a triplet state, as shown in Figure 5.

According to the extended transition state method,[30] the M–CH_2 bonding energy (*BE*) can be formally partitioned into the following terms

$$BE = -(\Delta E_{prep} + \Delta E_{st} + \Delta E_{orb})$$

The preparation energy term, ΔE_{prep}, is the energy difference between the ground state equilibrium geometry of each fragment and the geometry and electronic state they have in the complex. ΔE_{st}, is the steric energy term and represents the interaction energy between both prepared fragments with the geometries corresponding to the final complex, but with the densities that each fragment would have if the other fragment was absent. Finally, the orbital interaction term, ΔE_{orb}, takes into account the stabilization produced when the densities of both fragments are allowed to relax.

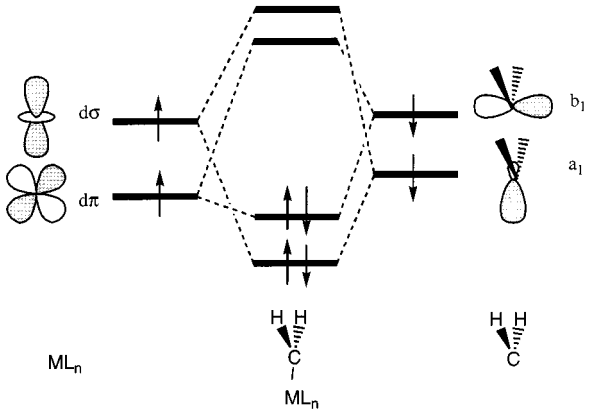

Figure 5. Schematic orbital interaction diagram for triplet methylene and a metal fragment

The formation of the M–CH_2 bond requires monooccupied dσ and dπ orbitals in the metal. These orbitals are doubly occupied in the ground state structure of **m-1**, where the only vacant metal d orbital is the one pointing to the four oxygen atoms (d_{xy}). In the prepared fragment, this orbital is doubly occupied, so that the interaction with the formate ligands becomes repulsive. Geometry distortion relieves this repulsion, leading to the structure shown in Figure 3.

For the metal fragment of **d-5**, the dσ orbital is the unoccupied antibonding combination of the Rh dz^2 orbitals, while dπ is the doubly occupied antibonding combination of the corresponding Rh d orbitals. The preparation of the metal fragment involves a promotion from dπ to dσ. Since dσ is a Rh–Rh antibonding orbital, the Rh–Rh bond becomes weaker upon complex formation (see Table 1 and Figure 3).

We separated the orbital interaction term into two contributions:

$$\Delta E_{orb} = \Delta E_{\sigma+\pi} + \Delta E_{pol}$$

The first term arises from a calculation in which all virtual orbitals of both fragments were removed, so that the energy stabilization is due only to the metal–carbene double bond formation. σ and π contributions can be separated, since the corresponding orbitals belong to different symmetry species, both in **m-3** (*a* and *b*) and in **d-5** (a_1 and b_1). The second term (ΔE_{pol}) is the additional stabilization produced when all virtual orbitals are included in the calculation and can be attributed to the polarization of the densities of both fragments.

Table 4 shows that the M–CH_2 bonds in **m-3** and **d-5** are weaker than in Cl_4WCH_2. The energy partition analysis shows that the dominant factor is the strength of σ and π interactions. The M–CH_2 bond is polarized towards

methylene. The Mulliken population analysis shows that the charge in the CH_2 fragment is –0.33 for **m-3** and –0.39 for **d-5**. The value obtained for Cl_4WCH_2 is –0.45, so that the donor ability of the metal fragments in **m-3** and **d-5** is lower than that of WCl_4.

Table 4. Components of the M–CH_2 bonding energy of metal–carbene complexes. See text for definitions; energies in kcal mol^{-1}

	Cl_4WCH_2	m-3	d-5
ΔE_{prep}	36.3	30.8	23.2
ΔE_{Pauli}	261.1	215.6	190.8
ΔE_{elstat}	–186.5	–150.2	–126.8
ΔE_{st}	74.6	65.4	64.0
ΔE_{σ}	–113.3	–95.0	–91.7
ΔE_{π}	–48.7	–34.0	–22.3
$\Delta E_{\sigma+\pi}$	–160.0	–129.0	–114.0
ΔE_{pol}	–36.6	–22.9	–26.5
BE	85.7	55.7	53.3

Since the M–CH_2 bond in **m-3** and **d-5** is not strong enough, these complexes are unstable with respect to methylene insertion in one of the M–O bonds. This process, which restores the square-planar coordination arrangement around the metal, involves the cleavage of a M–O bond and the formation of a σ M–C bond. For dimeric and trimeric palladium diformate, metal–carbene complexes are much more destabilized and do not correspond to stable structures. In these cases, the preparation energy of the metal fragment would be notably larger than for **m-3** and **d-5** and the rigidity of the structures does not allow a similar geometry relaxation as the one observed for the monomer.

We have seen that trimeric palladium diformate is thermodynamically stable with respect to fragmentation. Let us now consider the fragmentation of the methylene-inserted structure **t-4a**. This fragmentation can take place through the following steps:

t-4a → **d-1** + **m-4** (3)

t-4a → **d-4** + **m-1** (4)

d-4 → **m-4** + **m-1** (5)

Table 5. Variation of energy and thermodynamic functions for the fragmentation of **t-4a**

Step	ΔE[a]	$\Delta H°_{298}$[a]	$\Delta S°_{298}$[b]	$\Delta G°_{298}$[a]
3	4.3	2.6	39.2	–9.1
4	17.9	17.0	42.3	4.4
5	14.5	12.8	45.8	–0.9

[a] In kcal mol^{-1}. – [b] In cal K^{-1} mol^{-1}.

Table 5 contains the energies and variation of thermodynamic functions associated with these processes. Fragmentation is energetically unfavorable, but the inclusion of the entropy contribution makes step 3 thermodynamically favorable. These results can be compared with those corresponding to the fragmentation of **t-1** (Table 2), which was unfavorable even when the entropy contribution was considered.

Thus, **t-4a** is unstable with respect to fragmentation even in the gas phase and the monomeric **m-4** complex, which would be the product of such a process, could be envisaged as an intermediate in the cyclopropanation mechanism. A possible mechanistic scheme for the reaction between diazomethane and ethylene catalyzed by palladium dicarboxylates is presented in Figure 6. In the first step, the reaction between diazomethane and **t-1** leads to the formation of **t-4a**. Then, the fragmentation of this complex leads to **m-4**. Reaction between this complex and ethylene would lead to the formation of the corresponding cyclopropane derivative and **m-1**, which could also react with diazomethane to regenerate **m-4**. The reaction between **m-4** and the olefin is expected to involve several steps, such as the coordination of the olefin to Pd and the formation of a metalacyclobutane intermediate. The detailed study of this process, including the location of transition states, is currently in progress. The computed Gibbs energies presented in Figure 6 show that the overall mechanism is thermodynamically feasible for the cyclopropanation of ethylene.

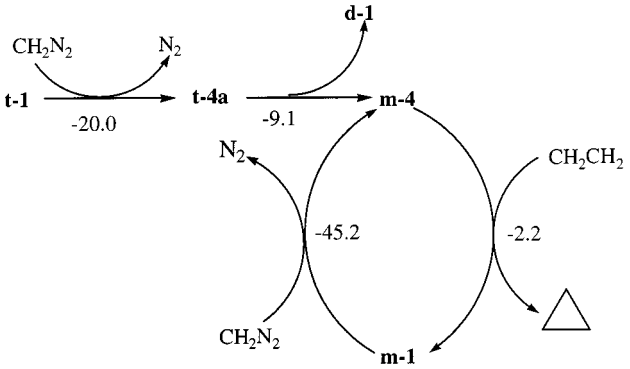

Figure 6. Possible mechanism for cyclopropanation of ethylene by diazomethane catalyzed by palladium diformate; values of reaction Gibbs energies are given in kcal mol^{-1}

As we mentioned in the introduction, other mechanisms involving the prior coordination of the olefin to palladium diacetate had also been postulated.[4] Our results showed that the coordination of an additional ligand in a tetracoordinated Pd^{II} complex requires an important rearrangement of the ligands to minimize metal–ligand repulsion. We saw that this rearrangement is not possible for the coordination of methylene in dimeric and trimeric palladium complexes. Similar behavior is expected for other ligands such as ethylene. So, a palladium–ethylene complex would only be formed from the monomeric structure **m-1**. We optimized the geometry of this complex and the obtained structure is shown in Figure 7. This structure can be consid-

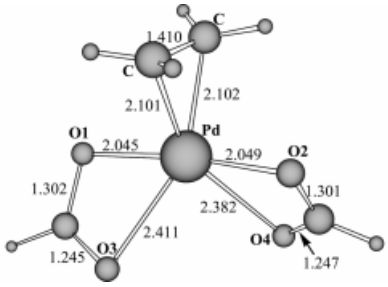

Figure 7. Structure of complexes arising from the interaction between ethylene and monomeric palladium diformate; distances are in Å

ered to be trigonal bipyramidal with ethylene in one of the equatorial positions. Compared to **m-4** (Figure 2), the Pd–O3 and Pd–O4 distances are notably larger in the ethylene complex, while Pd–O1 and Pd–O2 distances are slightly shorter. The computed Pd–ethylene bond dissociation energy is 16.8 kcal mol^{-1}. We also optimized the geometry of a complex in which ethylene inserts in one of the Pd–O bonds, but it is 2.7 kcal mol^{-1} higher in energy than the ethylene-coordinated complex.

The reaction between **m-1** and diazomethane to yield **m-4** and N_2 has a reaction energy of –47.2 kcal mol^{-1}, so that it is energetically much more favorable than the formation of the ethylene-coordinated complex. Cui et al.[31] studied the reaction between Cu and diazomethane to form $CuCH_2$ and N_2 theoretically, and observed that the reaction proceeds without an energy barrier and with a reaction energy of –34.9 kcal mol^{-1}. The formation of **m-4** from **m-1** and diazomethane involves an important rearrangement of the formate ligands, so that an energy barrier is expected for this process. Since this rearrangement is also necessary for ethylene coordination, the corresponding energy barriers are expected to be similar.

These results suggest that the mechanism for the cyclopropanation of olefins by diazomethane catalyzed by palladium dicarboxylates does not involve the prior formation of a metal–olefin complex. On the other hand, metal–carbene complexes are unstable with respect to methylene insertion in one of the Pd–O bonds, so that these CH_2-inserted species could be intermediates in the cyclopropanation mechanism.

Concluding Remarks

We optimized the geometries of several complexes arising from the interaction between methylene and palladium and rhodium diformates. In all cases, the most stable structures correspond to complexes in which methylene has inserted into one of the M–O bonds, while metal–carbene complexes correspond to energy minima only for monomeric palladium diformate and for dimeric rhodium diformate. In these cases, the analysis of the metal–carbene bonding shows that the bond is weaker than for other complexes, such as Cl_4WCH_2, due to a lower σ and π donor ability of the metal fragment.

Trimeric palladium formate (**t-1**) is thermodynamically stable upon fragmentation. However, when it forms a complex with methylene (**t-4a)**, fragmentation becomes favorable. The resulting monomeric complex **m-4** can be envisaged as an intermediate in the olefin cyclopropanation mechanism catalyzed by palladium dicarboxylates.

Acknowledgments

This work has been financially supported by DGESIC (PB97–0214). Computer time from Centre de Supercomputació de Catalunya (CESCA) and a doctoral fellowship from the Universitat Autònoma de Barcelona to C. R. are gratefully acknowledged. Finally, the authors thank Dr. Gabriel Aullón for helpful discussions on dimeric Pd^{II} complexes.

[1] M. P. Doyle, *Chem. Rev.* **1986**, *86*, 919.
[2] M. P. Doyle in: *Comprehensive Organometallic Chemistry 2, Vol 12* (Eds.: E. W. Abel, F. G. A. Stone, G. Wilkinson), Pergamon, New York, **1995**, p. 387.
[3] J. Pfeiffer, K. H. Dötz, *Angew. Chem. Int. Ed. Engl.* **1997**, *36*, 2828.
[4] A. J. Anciaux, A. J. Hubert, A. F. Noels, N. Petiniot, P. Teyssié, *J. Org. Chem.* **1980**, *45*, 695.
[5] R. M. Ortuño, J. Ibarzo, A. Alvarez-Larena, J. F. Piniella, *Tetrahedron Lett.* **1996**, *37*, 4059.
[6] D. Spangler, J. J. Wendolowski, M. Dupuis, M. M. L. Chen, H. F. Schaeffer III, *J. Am. Chem. Soc.* **1981**, *103*, 3985.
[7] [7a] H. Nakatsuji, J. Ushio, S. Han, T. Yonezawa, *J. Am. Chem. Soc.* **1983**, *105*, 426. – [7b] J. Ushio, H. Nakatsuji, T. Yonezawa, *J. Am. Chem. Soc.* **1984**, *106*, 5892.
[8] T. E. Taylor, M. B. Hall, *J. Am. Chem. Soc.* **1984**, *106*, 1576.
[9] M. Sodupe, J. M. Lluch, A. Oliva, J. Bertrán, *Organometallics* **1989**, *8*, 1837.
[10] T. R. Cundari, M. S. Gordon, *J. Am. Chem. Soc.* **1991**, *113*, 5231.
[11] A. Márquez, J. Fernandez Sanz, *J. Am. Chem. Soc.* **1992**, *114*, 2903.
[12] [12a] H. Jacobsen, G. Schreckenbach, T. Ziegler, *J. Phys. Chem.* **1994**, *98*, 11406. – [12b] H. Jacobsen, T. Ziegler, *Inorg. Chem.* **1996**, *35*, 775.
[13] S. Vyboishchikov, G. Frenking, *Chem. Eur. J.* **1998**, *4*, 1428.
[14] A. D. Becke, *Phys. Rev. A* **1988**, *38*, 3098.
[15] [15a] Y. Wang,. J. P. Perdew, *Phys. Rev. B* **1991**, *44*, 13298. – [15b] J. P. Perdew, J. A. Chevary, S. H. Vosko, K. A. Jackson, M. R. Pederson, D. J. Singh, C. Fiolhais, *Phys. Rev. B* **1992**, *46*, 6671.
[16] ADF 2.3, Theoretical Chemistry, Vrije Universiteit, Amsterdam.
[17] E .J. Baerends, D. E. Ellis, P. Ros, *Chem. Phys.* **1973**, *2*, 41.
[18] G. te Velde, E. J. Baerends, *J. Comp. Phys.* **1992**, *99*, 84.
[19] P. Vernooijs, G. J. Snijders, E. J. Baerends, *Slater Type Basis Functions for the Whole Periodic System*; Internal Report: Vrije Universiteit Amsterdam, The Netherlands, 1981.
[20] P. E. M. Siegbahn, *Chem. Phys. Lett.* **1993**, *201*, 15.
[21] T. Ziegler, V. Tschinke, E. J. Baerends, J. Snijders, W. Ravenek, *J. Phys. Chem.* **1989**, *93*, 3050.
[22] [22a] O. Gunnarsson, I. Lundquist, *Phys. Rev.* **1974**, *B10*, 1319. – [22b] S. H. Vosko, L. Wilk, M. Nusair, *Can. J. Phys.* **1980**, *58*, 1200.
[23] M. J. Frisch, G. W. Trucks, H. B. Schlegel, G. E. Scuseria, M. A. Robb, J. R. Cheeseman, V. G. Zakrzewski, J. A. Montgomery, Jr., R. E. Stratmann, J. C. Burant, S. Dapprich, J. M. Millam, A. D. Daniels, K. N. Kudin, M. C. Strain, O. Farkas, J. Tomasi, V. Barone, M. Cossi, R. Cammi, B. Mennucci, C. Pomelli, C. Adamo, S. Clifford, J. Ochterski, G. A. Petersson, P. Y. Ayala, Q. Cui, K. Morokuma, D. K. Malick, A. D. Rabuck, K. Raghavachari, J. B. Foresman, J. Cioslowski, J. V. Ortiz, B. B. Stefanov, G. Liu, A. Liashenko, P. Piskorz, I. Komaromi, R. Gomperts, R. L. Martin, D. J. Fox, T. Keith, M. A. Al-Laham, C. Y. Peng, A. Nanayakkara, C. Gonzalez, M. Challacombe, P. M. W. Gill, B. Johnson, W. Chen, M. W. Wong, J. L. Andres, C. Gonzalez, M. Head-Gordon, E. S. Replogle, J. A. Pople, *Gaussian 98*, Revision A.5; Gaussian, Inc.: Pittsburgh PA, **1998**.
[24] P. J. Hay, W. R. Wadt, *J. Chem. Phys.* **1985**, *82*, 299.
[25] T. H. Dunning Jr., P. J. Hay in: *Modern Theoretical Chemistry*, *Vol 3* (Ed.: H. F. Schaeffer III), Plenum, New York, **1976**, p. 1.
[26] [26a] F. A. Cotton, S. Han, *Rev. Chim. Minerale.* **1983**, *20*, 496. – [26b] D. H. R. Barton, J. Khamsi, N. Ozbalik, M. Ramesh, J. C. Sarma, *Tetrahedron Lett.* **1989**, *30*, 4661.
[27] F. A. Cotton, B. G. DeBoer, M. D. LaPrade, J. R. Pipal, D. A. Ucko, *Acta Crystalogr.* **1971**, *B27*, 1664.
[28] F. A. Cotton, X. Feng, *J. Am. Chem. Soc.* **1998**, *120*, 3387.
[29] G. Aullón, P. Alemany, S. Alvarez, *Inorg. Chem.* **1996**, *35*, 5061, and references therein.
[30] T. Ziegler, A. Rauk,. *Theoret. Chim. Acta* **1977**, *46*, 1.
[31] Q. Cui, D. G. Musaev, M. Svensson, K. Morokuma, *J. Phys. Chem.* **1996**, *100*, 10936.

Received November 9, 1999
[I99397]